JBIC (1999) 4:692–700

ORIGINAL ARTICLE

Elena Babini · Marco Borsari · Francesco Capozzi
Lindsay D. Eltis · Claudio Luchinat

Experimental evidence for the role of buried polar groups in determining the reduction potential of metalloproteins: the S79P variant of *Chromatium vinosum* HiPIP

Received: 26 April 1999 / Accepted: 24 August 1999

Abstract The amide group between residues 78 and 79 of *Chromatium vinosum* high-potential iron-sulfur protein (HiPIP) is in close proximity to the Fe_4S_4 cluster of this protein and interacts via a hydrogen bond with Sγ of Cys77, one of the cluster ligands. The reduction potential of the S79P variant was 104 ± 3 mV lower than that of the recombinant wild-type (rcWT) HiPIP (5 mM phosphate, 100 mM NaCl, pH 7, 293 K), principally due to a decrease in the enthalpic term which favors the reduction of the rcWT protein. Analysis of the variant protein by NMR spectroscopy indicated that the substitution has little effect on the structure of the HiPIP or on the electron distribution in the oxidized cluster. Potential energy calculations indicate that the difference in reduction potential between rcWT and S79P variant HiPIPs is due to the different electrostatic properties of amide 79 in these two proteins. These results suggest that the influence of amide group 79 on the reduction potential of *C. vinosum* HiPIP is a manifestation of a general electrostatic effect rather than a specific interaction. More generally, these results provide experimental evidence for the importance of buried polar groups in determining the reduction potentials of metalloproteins.

Key words *Chromatium vinosum* · Electrostatic effects · High-potential iron-sulfur protein · NMR spectroscopy · Reduction potential

E. Babini
Food Science Laboratory, University of Bologna
Via Ravennate 1020, I-47023 Cesena (FO), Italy

M. Borsari
Department of Chemistry, University of Modena
Via Campi 183, I-41100 Modena, Italy

F. Capozzi
Department of Chemistry, University of Calabria, P. Bucci
I-87030 Arcavacata di Rende (CS), Italy

L.D. Eltis
Department of Biochemistry, Université Laval, Quebec City
Quebec G1K 7P4, Canada

C. Luchinat (✉)
Department of Soil Science and Plant Nutrition, University of Florence, P.le delle Cascine 28, I-50144 Florence, Italy, and
Centro Risonanze Magnetiche, Via L. Sacconi 6,
I-50019 S.to Fiorentino (Florence), Italy
e-mail: luchinat@cerm.unifi.it
Tel.: +39-55-2388200/4209262
Fax: +39-55-333273/4209253

Introduction

The factors determining the reduction potentials of metalloproteins have been assessed by experimental and theoretical approaches. The intrinsic redox properties of the metal center are modulated by the endogenous ligands provided by the protein and are further tuned by the protein environment, principally through electrostatic effects [1–8]. These electrostatic effects include unitary charges of acidic and basic residues and partial charges of protein polar groups [1, 5, 7, 9–11]. Although unitary charges are larger than partial charges, they are usually located at the protein's surface and are thus shielded by the solvent dielectric. In contrast, partial charges, which are more numerous, are often buried within the protein and are thus not shielded by the solvent. Several theoretical studies have stressed the importance of buried partial charges in determining the reduction potential of metalloproteins [1, 8, 12]. Experimental evidence has been less forthcoming, although it has recently been reported that the elimination of polar side chains that hydrogen bond to the Rieske Fe_2S_2 cluster of the cytochrome bc_1 complex decreases the reduction potential of this cluster by 50–130 mV [13, 14].

The study of high-potential iron-sulfur proteins (HiPIPs) has provided many important insights into the control of reduction potential in metalloproteins [1, 5]. These small, soluble proteins contain a Fe_4S_4 cluster bound to the polypeptide by four cysteinyl thiolate li-

gands. The functional oxidation states of the cluster are $[(RS)_4Fe_4S_4]^-$ and $[(RS)_4Fe_4S_4]^{2-}$ and the reduction potential of this redox couple ranges from 90 to 500 mV. In contrast, the functional oxidation states of the Fe_4S_4 cluster-containing ferredoxins (Fds) are $[(RS)_4Fe_4S_4]^{2-}$ and $[(RS)_4Fe_4S_4]^{3-}$ and their reduction potentials range from -400 to -650 mV [5]. The existence of different redox couples in HiPIPs and Fds complicates a direct comparison of their reduction potentials. However, Hagen and co-workers [15] recently "superreduced" the HiPIP of *Rhodophila globiformis* to the $[(RS)_4Fe_4S_4]^{3-}$ state, determining the reduction potential of the $[(RS)_4Fe_4S_4]^{2-/3-}$ couple to be –900 mV. This potential is about 1.35 V lower than that of the $[(RS)_4Fe_4S_4]^{2-/3-}$ couple in the same protein and suggests that the reduction potential of the $[(RS)_4Fe_4S_4]^{2-/3-}$ couple in HiPIPs is in the range -850 to -1250 mV, i.e. about 400–600 mV lower, on the average, than in the Fds.

The considerable difference in reduction potential between HiPIPs and Fds has been explained by the larger solvent exposure of the cluster in Fds and by the larger number of positive partial charges surrounding the ferredoxin cluster [1, 5]. Warshel and co-workers [1] have attributed a particularly significant role to the main-chain amide groups. Ferredoxins contain 15 such groups within 10 Å of the centroid of the cluster, 13 of which are oriented with their positive end towards the cluster. In contrast, HiPIPs contain eight such groups within 10 Å of the centroid of the cluster, seven of which are oriented with their positive end towards the cluster [1]. This model extends the original concepts of Carter et al. [17] and Sanders-Loehr and co-workers [16], who suggested that the difference between the two classes of Fe_4S_4 cluster-containing proteins is due to the different number of hydrogen bonds between main-chain amide groups and the cluster sulfur atoms (five in HiPIPs versus eight in Fds), as well as the more hydrophobic nature of the cluster environment in HiPIPs, although the contribution of surface charges is not negligible in proteins where the cluster is less solvent exposed [18].

The role of main-chain amide groups in modulating the reduction potential of metalloproteins is difficult to assess by mutagenic approaches. One approach is to substitute residues participating in key amide bonds with proline. This eliminates the capacity of the peptide bond to donate a hydrogen bond and distributes the partial positive charge over the Cδ and the δ-CH_2 protons of the proline residue. In the current study, serine 79 of *Chromatium vinosum* HiPIP was substituted with proline. Amide 79 forms a hydrogen bond to Sγ of Cys77, one of the cluster ligands, and was identified as being "especially important" by Warshel and co-workers [1]. This residue was targeted since the φ angle of Ser79 indicated that the introduction of a proline at this position would not alter the overall folding of the protein. Indeed, one of the major problems in using mutations to prove or disprove working hypotheses in proteins is to ascertain that the mutation has no other sizable effects besides the predicted one. This is even more crucial with mutations to proline, which locally rigidifies the backbone and may cause steric constraints that may propagate as gross torsion angle alterations along the backbone, giving undesired effects. Fortunately, the presence of the paramagnetic cluster allows us to observe by ^{1}HNMR the hyperfine shifted signals of all cysteine protons [19]. Hyperfine shifts are very sensitive to even minor alterations of the coordination environment, and their changes are faithful reporters of the kind of alteration. The S79P variant was purified to apparent homogeneity and its reduction potential was determined. The effects of the substitution on the structure of the protein and the electron distribution of the oxidized cluster were assessed by NMR spectroscopy. Potential energy calculations were performed to evaluate the origin of the observed difference in the reduction potentials of wild-type and S79P variant HiPIPs.

Materials and methods

All chemicals were of the highest quality available. All buffers were made with water purified to a resistivity of 15 MΩ cm using a Millipore Elix 5 water purification apparatus.

DNA manipulation and protein purification

DNA was manipulated using standard protocols [20]. Oligonucleotide-directed mutagenesis was performed using a uracil-containing single-stranded template [21]. The template was prepared from the plasmid pEBCV10 which contains a synthetic gene encoding a histidine-tagged *C. vinosum* HiPIP [22]. The mutagenesis reaction was performed using the oligonucleotide 5′-AGA GTC CAC G**G**A GCG CAC CAG-3′ in which the mismatched nucleotide is in bold-faced type. The nucleotide sequence of the gene encoding the S79P variant was verified.

Recombinant wild-type (rcWT) and S79P variant *C. vinosum* HiPIPs were expressed and purified essentially as previously described [23]. Proteins for spectrophotometry and electrochemistry were prepared in 50 mM potassium phosphate (pH 7.4). Protein samples were prepared for NMR experiments by diluting them 10-fold with deuterated 50 mM potassium phosphate (pH 7.4) and concentrating them by ultrafiltration using an Amicon cell equipped with a YM5 membrane. This procedure was repeated four times. Oxidized proteins were prepared by adding a slight molar excess of $[Fe(CN)_6]^{3-}$ in deuterated solution to the samples.

UV-visible absorption spectroscopy

UV/vis spectra were recorded using a Shimadzu UV-1200 spectrophotometer equipped with a thermostatted cuvette holder. Spectra were recorded between 250 and 600 nm at 298 K. The concentration of HiPIP was determined using an extinction coefficient of 16.1 mM^{-1} cm^{-1} at 388 nm for the fully oxidized protein [24].

Cyclic voltammetry

Cyclic voltammetry (CV) was performed using a Princeton Applied Research model 273A potentiostat/galvanostat and a small-volume cell (0.5 ml). A 2 mm diameter highly oriented pyrolytic

graphite disc was used as the working electrode, a platinum sheet served as the counter electrode and the reference electrode was a saturated calomel electrode (SCE). Immediately prior to each CV experiment, the working electrode was cleaned by soaking it in ethanol for 10 min, polishing it with an alumina-water slurry (BDH, particle size ~0.015 μm) on cotton wool, then treating it in an ultrasonic bath for approximately 10 min. Voltammograms were recorded at different scan rates (20–200 mV/s). Potentials were calibrated using the methylviologen^{2+}/methylviologen^{+} couple and were recalculated with respect to the standard hydrogen electrode (SHE).

Protein samples were prepared immediately prior to the experiment from a 1 mM stock solution containing 50 mM potassium phosphate (pH 7) and 150 mM KCl. The HiPIP was diluted to a final concentration of 0.1 mM in 0.50 ml containing 0.1 M NaCl as a base electrolyte, and 8 mM morpholine and 0.7 mM poly-l-lysine as promoters. The pH was adjusted to the desired value with solutions of concentrated NaOH or HCl and was measured before and after the electrochemical experiment. The sample was maintained under argon during the experiment. The temperature dependence of the reduction potential was determined using a non-isothermal configuration in which the reference electrode was kept at constant temperature (298 K) and the temperature of the electrochemical cell was varied [25]. The reduction potentials determined from replicate experiments agreed within 2 mV.

NMR spectroscopy

NMR spectra were recorded at 290 or 305 K using a Bruker Avance 800 MHz spectrometer operating at a magnetic field of 18.79 T. The two-dimensional NOESY experiments were performed at 290 K using a spectral window of 190 kHz, a mixing time of 25 ms (for the oxidized form) or 10 ms (for the reduced form) and a recycle delay of 300 ms. Data were collected over 2048 points in the acquisition dimension at each of 128 increments. Raw data were processed used a cosine-squared filter function in both dimensions and a polynomial baseline correction was applied, also in both dimensions. Data were zero-filled to obtain a matrix of 2k × 2k data points. Chemical shifts were calibrated by assigning a value of $\delta = 5.11–0.012T$ to the residual water signal, where T is the probe temperature in °C. The saturation transfer experiment was performed on a mixture of 1:2 oxidized:reduced forms, using a mixing time of 5 ms, and by processing the two-dimensional spectrum with the same parameters used for the NOESY spectra.

Electrostatic calculations

Energy minimizations and calculations were performed using the SANDER module of the AMBER package [26]. The initial structural coordinates were obtained from the X-ray crystallographic structure of the oxidized rcWT HiPIP determined to 1.20 Å [27]. The coordinates of the S79P variant HiPIP were obtained by substituting Ser79 in the crystallographic structure of the oxidized rcWT HiPIP with proline using the program MOLMOL [28]. The partial charges of the atoms in the oxidized cluster were assigned according to each of three previously defined configurations: OS1, OS2 and OS3 [29]. The partial charges of the atoms in the reduced cluster were assigned by distributing a single negative charge over the atoms of the oxidized Fe_4S_4 cluster and some ligand atoms. The partial charges assigned to cluster and ligand atoms are reported in Table 1. The potential energy of all structures was minimized using a distance-dependent dielectric function (i.e. idiel = 0) and $\varepsilon = 1$ to mimic the presence of solvent, since no explicit water was included in the structures. Minimization to a convergence criterion of 0.2 kcal/mol was achieved using 1500 iterations of the method of steepest descent followed by the method of conjugate gradients [26, 30]. During this minimization, the short-range van der Waal's interactions were attenuated by setting the SCNB parameter to 100, thereby constraining the geometry of the cluster and its ligands.

Table 1 Partial charges assigned to the atoms of the cluster and its ligands and used in the energy minimization and potential energy calculations [26, 29]

Atom type	Reduced	Oxidized		
		OS1	OS2	OS3
N	−0.4157	−0.4157	−0.4157	−0.4157
HN	0.2719	0.2719	0.2719	0.2719
CA	0.0213	0.0213	0.0213	0.0213
HA	0.1124	0.1124	0.1124	0.1124
CB	0.0500	0.0865	0.0870	0.0880
HB2	0.1112	0.1112	0.1112	0.1112
HB3	0.1112	0.1112	0.1112	0.1112
SG	−0.5670	−0.4135	−0.3995	−0.4175
LP1	−0.12035	−0.12085	−0.11385	−0.12110
LP2	−0.12035	−0.12085	−0.11385	−0.12110
C	0.5973	0.5973	0.5973	0.5973
O	−0.5679	−0.5679	−0.5679	−0.5679
Fe	0.4090	0.3125	0.2980	0.3345
S	−0.3930	−0.2355	−0.2495	−0.2545

The potential energies of each minimized structure were calculated according to reported methodologies [26, 30]. For these calculations, a constant dielectric was used (i.e. idiel = 1) and ε was set to a value between 1 and 2. Potential energies were calculated by explicitly considering the following terms: *bond*, covalent interactions; *angle*, angular torsions; *dihed*, dihedral torsions; *elect*, electrostatic interactions between atoms separated by more than four covalent bonds; *(1–4)el*, electrostatic interactions between atoms separated by less than four covalent bonds; *vdW*, van der Waals interaction energy between atoms separated by more than four covalent bonds; *(1–4)NB*, van der Waals interactions between atoms separated by less than four covalent bonds; and *Hbond*, hydrogen-bonding interactions. The calculated energies were expressed as the difference between the potential energy of the reduced form and that of each oxidized form model (OS1–OS3).

Results and discussion

The electronic absorption spectra of rcWT and S79P variant HiPIP were essentially identical (results not shown) and the *R*-factors (A_{280}/A_{388}) of the freshly oxidized rcWT and S79P variant HiPIPs were 2.58 and 2.63, respectively. These results and the NMR data (see below) indicate that the Fe_4S_4 cluster was not grossly altered in the variant HiPIP. Moreover, the S79P variant was of comparable stability to the rcWT in solution at room temperature, indicating that the protein fold was not perturbed in such a way as to expose the Fe_4S_4 cluster to solvent [31, 32].

The reduction potential of the S79P variant and rcWT HiPIPs were 251 ± 2 mV and 355 ± 2 mV, respectively, versus SHE (~5 mM potassium phosphate, 0.1 M NaCl, pH 7.0, 293 K). In agreement with previous reports [33], the reduction potential of the rcWT HiPIP was essentially independent of pH above pH 7 and increased at lower pH with an apparent pK_a of approximately 5.7 due to the protonation of His42 (Fig. 1a).

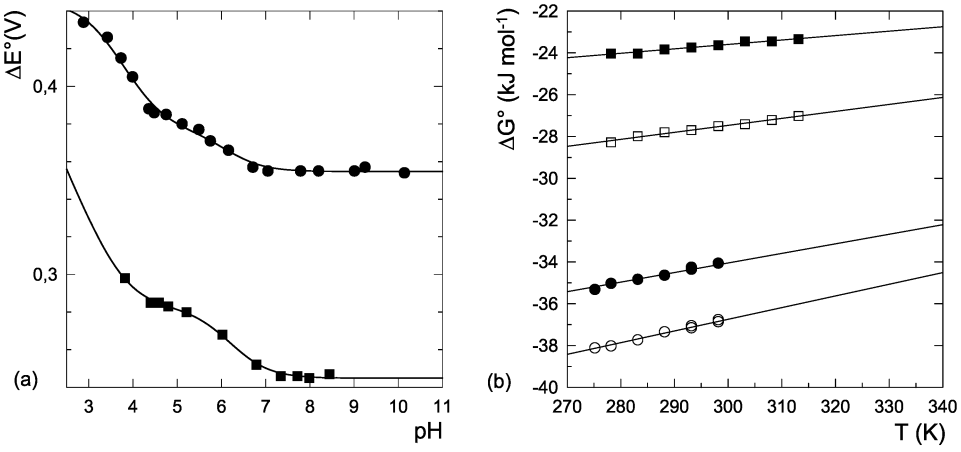

Fig. 1 **a** The reduction potential of rcWT (●) and S79P variant (■) *C. vinosum* HiPIPs as a function of pH, determined at 293 K. $\Delta E°$ are reported relative to the standard hydrogen electrode (SHE). **b** The temperature dependences of the standard Gibbs free energy ($\Delta G°$) for the reduction of rcWT HiPIP at pH 4.75 (○) and at pH 8.21 (●), and of the S79P variant at pH 4.29 (❑) and at pH 7.34 (■)

The further increase of the reduction potential at lower pH was presumably due to the protonation of Glu and Asp residues [33]. The reduction potential of S79P mutant displayed a very similar pH dependence except that the former was consistently 90–110 mV lower than that of the rcWT (Fig. 1a). The differences in the reduction potentials of S79P and rcWT were thus essentially independent of pH.

The temperature dependence of the reduction potentials of S79P variant and rcWT HiPIPs, determined at two different pH values, are reported as $\Delta G°$ values in Fig. 1b. The $\Delta H°$ and $\Delta S°$ at 298 K were evaluated from the slopes and intercepts of these data (Table 2). As has already been reported, the reduction of rcWT HiPIP at room temperature consists of a favorable enthalpic component and a smaller, unfavorable entropic component [25]. The position 79 substitution decreased the favorable enthalpic component by an amount equivalent to approximately 150 mV and decreased the unfavorable entropic component by an amount corresponding to an increase of 50 mV with respect to the potential of the rcWT. Both the enthalpic and the entropic effects of the position 79 substitution appeared to be essentially independent of pH.

The ^{1}H NMR spectra of the oxidized S79P variant and rcWT *C. vinosum* HiPIPs were very similar (Fig. 2, [34]). The hyperfine-shifted resonances of the former were assigned using the dipolar connectivities of the cysteine β-CH_2 protons to neighboring protons and the existing assignment and dipolar connectivities of the rcWT protein. Figure 3A shows an enlargement of a short-mixing NOESY spectrum of the oxidized S79P variant in which the connectivities of three hyperfine shifted resonances (b', d' and e') are highlighted. These connectivities are characteristic of the NOESY pattern of Cys77, which consists of an α-CH (e') and two β-CH_2 (b' and d') protons. This pattern closely matches that observed in the rcWT protein except for a switch of the resonances d' and b'. In all oxidized HiPIPs studied to date, Cys77 is the only cysteine ligand whose α-CH proton resonates well outside the diamagnetic region and therefore is the only cysteine that yields this three-spin pattern [35–37]. NOESY connectivities were also observed between resonances a' and c' and between resonances h' and i'. The assignment of these pairs of resonances, as well as that of resonances f' and g', was therefore completed by comparison with the rcWT spectrum (Fig. 2, [34]) and is summarized in Table 3 together with the temperature dependence of the resonances.

Table 2 Thermodynamic parameters of the reduction of rcWT and S79P *C. vinosum* HiPIPs

HiPIP	pH	$\Delta H°$ (kJ mol^{-1})	$\Delta S°$ (J mol^{-1} K^{-1})	$\Delta G°$[a] (kJ mol^{-1})	r (goodness of fit)
rcWT	8.21	−47.8	−45.7	−34.2	0.996
	4.75	−53.5	−55.8	−36.9	0.997
S79P	7.34	−29.9	−21.1	−23.6	0.984
	4.29	−37.5	−33.3	−27.6	0.986

[a] Values were determined at 298 K

The ^{1}H NMR spectra of the reduced *C. vinosum* rcWT and S79P HiPIPs were also similar (Fig. 4), except for a slight broadening of the whole spectrum observed for the reduced mutant protein. A possible explanation for this broadening could be that some protein loses its cluster, as the purity factor A_{280}/A_{390} increases from 2.5 to 2.75 in 16 h at 4 °C; iron ions released in solution by the cluster decomposition may be responsible of the observed signal broadening. The hyperfine shifted resonances, which have been assigned in the WT HiPIP and which arise from the β-CH_2 protons of the cysteine ligands [34], are sensitive probes of the Fe-S-C-H dihedral angles [38]. The full assignment of the β-CH_2 protons (Table 3) was performed by short mixing time NOESY. An enlargement of the NOESY spectrum is shown in Fig. 3B. From the resonance positions, the Fe-S-C-H dihedral angles of all cysteines except Cys77 are essentially the same. For Cys77, the reversal in shifts of its β-CH_2 protons, also observed in the oxidized form and confirmed by saturation transfer experiments (not shown), can be accounted for by a ro-

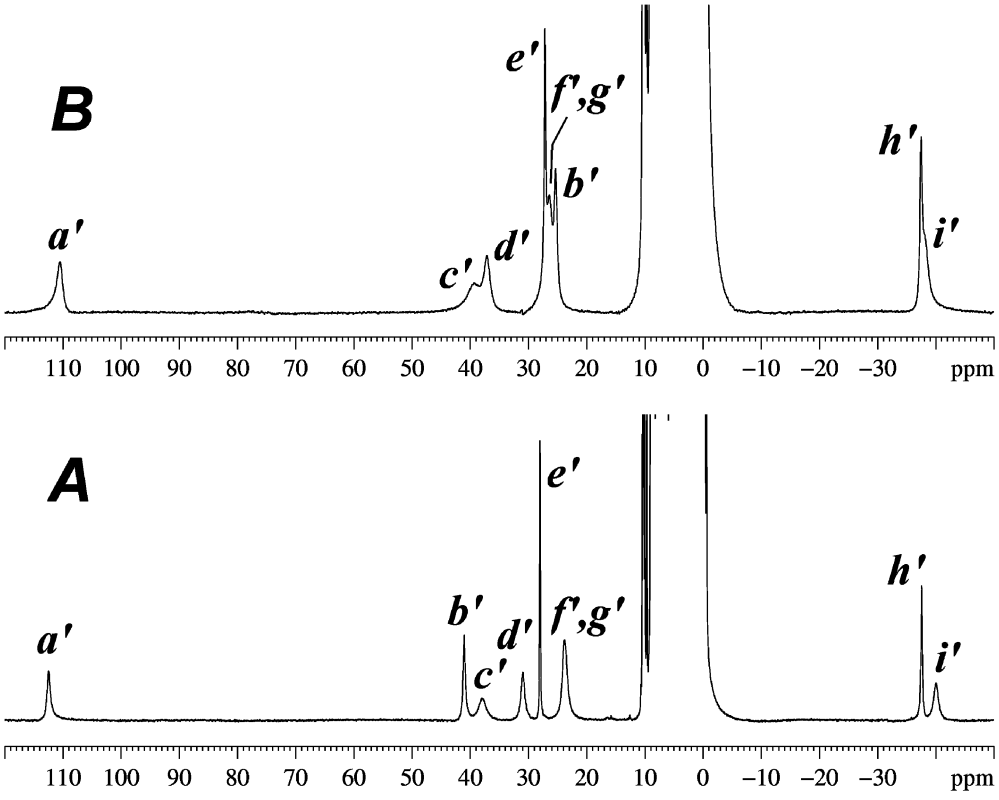

Fig. 2 800 MHz ^{1}HNMR spectra of oxidized rcWT (**A**) and S79P variant (**B**) *C. vinosum* HiPIPs. The spectra were recorded in 50 mM potassium phosphate/99.95% D_2O, pH 7.4, at 290 K. The assignments of resonances *a'* to *i'* are provided in Table 3

tation of approximately 30° about the S-Cβ axis, in such a way as to bring the Hβ_2 proton closer to a *trans* position with respect to the metal. This local change is not surprising in view of the loss of the H-bonding interaction between the sulfur atom and the NH group of residue 79.

The essential invariance of the dihedral angles of the other three coordinated cysteines suggests that it is unlikely that the introduction of proline at position 79 resulted in conformational changes remote from the site of substitution, for example through the propagation of constraints through main-chain torsion angles. Thus, the principal structural differences between the S79P variant and rcWT occur in the immediate vicinity of the substitution: the elimination of a hydrogen bond between backbone amide 79 and the Sγ of the Cys77 cluster ligand and the introduction of a less-polar side-chain at position 79. In the WT protein, the hydroxyl group of Ser79 is oriented towards the solvent such that its removal would be expected to slightly increase the reduction potential of the HiPIP [1]. Differences in the physicochemical properties of the S79P variant and

Table 3 Summary of the ^{1}HNMR assignments of the ligand proton resonances of rcWT and S79P *C. vinosum* HiPIP[a]

Residue	Proton	Oxidized			Reduced		
		Signal	Chemical shift (ppm)[b]		Signal	Chemical shift (ppm)[c]	
			RcWT	S79P		rcWT	S79P
Cys43	Hβ1	h'	−37.6 (pC)	−37.5 (pC)	y	7.5	8.0
	Hβ2	i'	−40.1 (pC)	−38.2 (pC)	a	16.4	16.3
Cys46	Hβ1	g'	23.6 (aC)	26.3 (aC)	e	10.0	10.8
	Hβ2	f'	23.8 (aC)	26.3 (aC)	d	11.0	11.5
Cys63	Hβ1	c'	37.8 (C)	39.3 (C)	z	5.5	5.2
	Hβ2	a'	112.4 (C)	110.4 (C)	b	15.7	14.9
Cys77	Hβ1[c]	b'	41.0 (C)	25.3 (C)	c	12.6	10.4
	Hβ2[c]	d'	30.9 (C)	37.0 (C)	w	7.8	12.9
	Hα	e'	27.9 (C)	27.1 (C)	v	8.4	8.9

[a] Labeling as in [34]
[b] Values were determined in 50 mM potassium phosphate/99.95% D_2O, pH 7.4, 290 K. Temperature dependence is indicated as: C, Curie; aC, anti-Curie; and pC, pseudo-Curie, as defined in [19]
[c] Correspondence between oxidized and reduced forms checked by saturation transfer

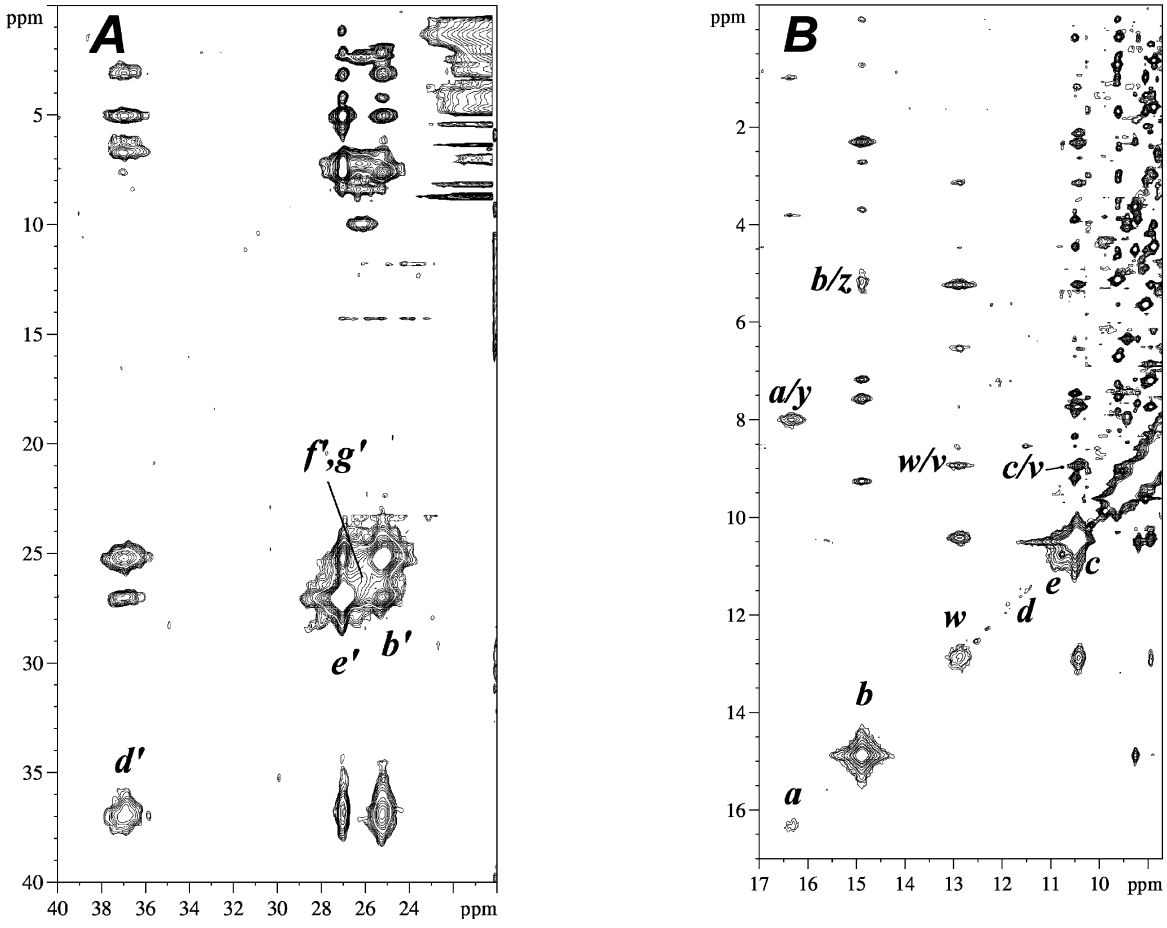

Fig. 3 800 MHz ^{1}HNOESY spectrum of oxidized (**A**) and reduced (**B**) S79P variant of *C. vinosum* HiPIP. These expanded regions highlight the connectivities between hyperfine shifted signals *b'*, *d'* and *e'* (*c*, *w* and *v*, in the reduced form), belonging to Cys77 Hβ_1, Hβ_2 and Hα, in that order. For the reduced form, the assignment of the other cysteine protons is also reported. The spectra were recorded in 50 mM potassium phosphate/99.95% D_2O, pH 7.4, at 290 K

rcWT HiPIPs can thus be ascribed to modification of the amide group 79.

In oxidized HiPIPs, the ferric versus mixed-valence character of each iron in the cluster, and thus their relative reduction potentials, can be estimated from the chemical shifts and temperature dependences of the hyperfine shifted resonances of the β-CH_2 protons of the cluster-ligating cysteines [39]. Inspection of Table 3 reveals that the substitution at position 79 shifted the β-CH_2 protons of Cys77 slightly upfield and shifted those of Cys46 slightly downfield with respect to those of the rcWT protein. The magnitude of these differences indicates that the iron bound to Cys77, which is 40% ferric in rcWT, was 45% ferric in the S79P variant and that the iron bound to Cys46, which is 60% ferric in rcWT, was 55% ferric in the S79P variant.

The effect of the position 79 substitution on the electron distribution of the cluster is therefore modest, and similar in magnitude to that of the modification of a surface charge. For example, the substitution of a single-charged surface residue in *Ectothiorhodospira halophila* HiPIP-I, which altered the reduction potential of this protein by up to 50 mV, altered the ferric character of individual irons by no more than 5 percentage points [3]. In contrast, the substitution of the cluster-ligating Cys77 of *C. vinosum* HiPIP with serine, which decreased the reduction potential by 25 mV, increased the ferric character of the iron ligated to residue 77 from 40% in oxidized rcWT to 55% in the oxidized C77S variant and decreased the ferric character of the iron ligated to residue 46 from 60% to 45% [22]. The effect of the substitution at position 79 on the microscopic reduction potentials of the individual cluster irons thus appears to be of a general electrostatic nature, despite the fact that amide 79 interacts specifically with the Cys77 ligand and that specific mutation of the latter residue significantly altered the microscopic reduction potential of the iron coordinated to that residue.

Coulomb's law predicts that electrostatic effects depend weakly on distance, varying with $1/r$ between the two charges. In this respect, the amide proton of Ser79 is 2.70 Å from the Sγ of Cys77, 4.32 Å from the iron bound to Cys77 and 8.30 Å from the farthest cluster atom, Sγ of Cys43. These distances differ by only a factor of three, indicating that the amide proton of Ser79

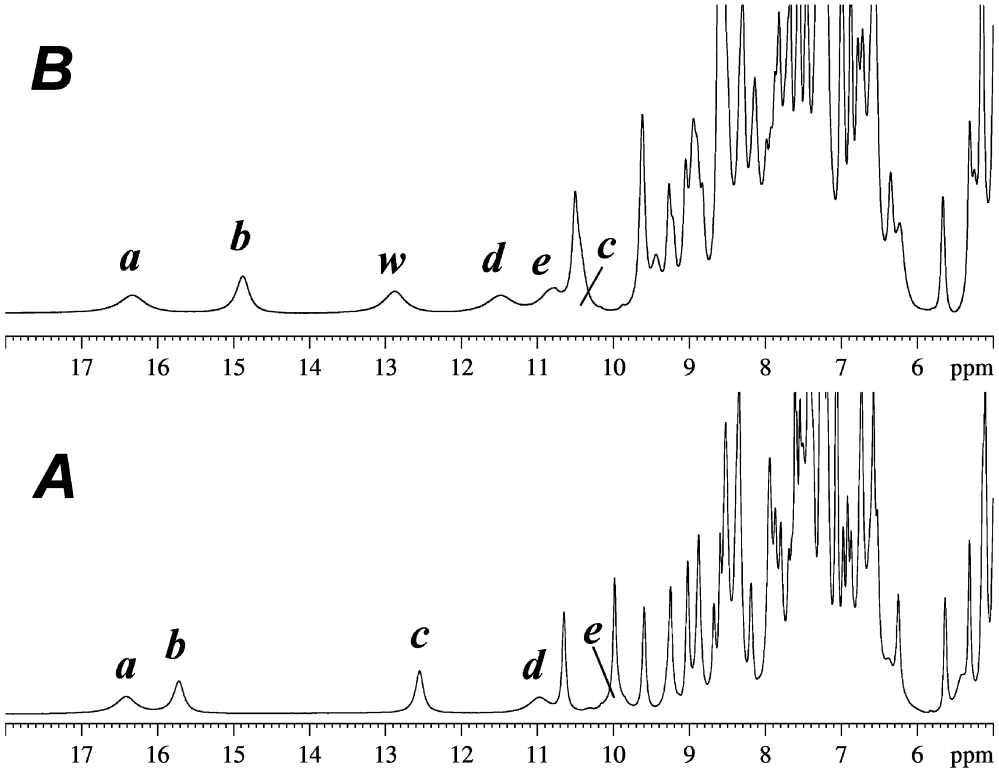

Fig. 4 800 MHz ^{1}H NMR spectra of reduced rcWT (**A**) and S79P variant (**B**) *C. vinosum* HiPIPs The spectra were recorded in 50 mM potassium phosphate/99.95% D_2O, pH 7.4, at 290 K. The assignments of the labeled resonances are provided in Table 3

could contribute to the stabilization of the additional negative charge on the reduced cluster regardless of the charge's precise distribution. However, it is difficult to quantitatively model electrostatic interactions in proteins owing to the effect of solvent and atomic motions within the protein. Atomic motions may cause the effective dielectric within the protein to vary from one region to another and to vary with distance [4, 40]. Despite these limitations, electrostatic effects can be calculated to within an order of magnitude using atomic resolution structures and estimates made of the partial charges of each protein atom.

An analysis of the calculated difference in potential energies, ΔE, between the oxidized and reduced HiPIPs revealed several interesting trends. Firstly, the overall calculated difference between the S79P variant and rcWT HiPIPs, $\Delta\Delta E_T$, did not depend strongly on the charge distribution used to model the oxidized cluster (Table 4). This finding is consistent with the NMR analysis of the S79P variant, which demonstrated that the modification of amide 79 did not significantly alter the electron distribution in the cluster, thereby supporting the conclusion that the effect of the substitution at position 79 does not result from the perturbation of an interaction with a specific cluster ligand. Secondly, regardless of the charge distribution of the oxidized cluster and the value of ε used in the calculation, the major influence of the substitution is on the electrostatic component of the potential energy. Moreover, the magnitude of this difference in the electrostatic energy compares favorably with the difference in enthalpic components of the respective reduction potentials of the rcWT and S79P variant HiPIPs (150 mV).

Table 4 Calculated differences in potential energy between rcWT and S79P variant *C. vinosum* HiPIPs[a]

	OS1/ε=1.0	OS2/ε=1.0	OS3/ε=1.0	OS3/ε=1.5	OS3/ε=2.0
$\Delta\Delta E_T$	−281.65	−214.58	−262.34	−163.13	−113.53
$\Delta\Delta E_{bond}$	2.27	−4.68	−0.37	−0.37	−0.37
$\Delta\Delta E_{(1-4)NB}$	−13.22	2.34	−9.28	−9.28	−9.28
$\Delta\Delta E_{elect}$	−351.65	−127.59	−290.66	−193.78	−145.33
$\Delta\Delta E_{angle}$	39.46	−24.60	18.77	18.77	18.77
$\Delta\Delta E_{(1-4)el}$	9.89	−65.34	−6.96	−4.64	−3.48
$\Delta\Delta E_{Hbond}$	7.07	18.41	7.37	7.37	7.37
$\Delta\Delta E_{dihed}$	7.85	−1.13	7.99	7.99	7.99
$\Delta\Delta E_{vdW}$	16.70	−11.99	10.80	10.80	10.80

[a] Calculations were performed as described in Materials and methods using three different charge distributions in the oxidized cluster (OS1–OS3) and three values of ε for the OS3 case [30]. The units are mV

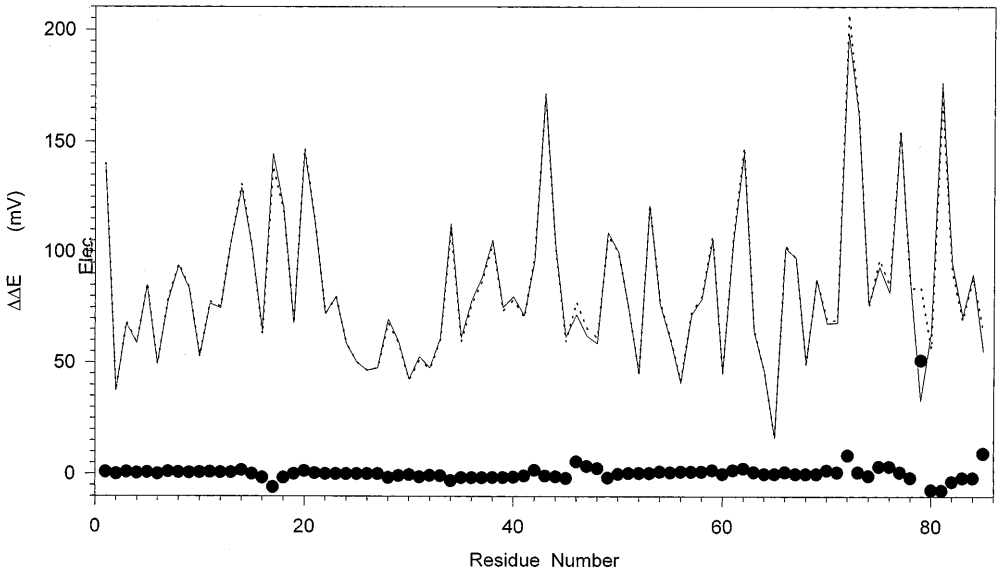

Fig. 5 The contribution of individual main-chain amides to the difference in electrostatic potential of reduced and oxidized *C. vinosum* HiPIPs. The symbols represent rcWT (---), S79P variant (——) and the difference between these two proteins (●). These data were obtained from a calculation using the OS3 oxidized model versus the reduced cluster charge distributions and a dielectric constant, ε, of 1

Evaluation of the contribution of each main-chain amide group to the electrostatic energy in the rcWT and S79P variant HiPIPs revealed that the major difference in this energy arises from the different contribution of amide 79 in the two proteins (Fig. 5). The magnitude of this difference depended on the partial charge assigned to the δC of Pro79, varying from 90 mV to 200 mV for partial charges of 0.097 and 0.019, respectively. The striking feature of these data is the relative magnitude of the difference of this contribution of amide 79 with respect to the differences of the contributions of the other main-chain amide groups. This suggests that the influence of the position 79 substitution arises from a direct effect and not an indirect one, such as might arise from a substitution-induced reorientation of other main-chain amide groups. These calculations thus indicate that the difference in reduction potential between rcWT and S79P variant HiPIPs is due to the different electrostatic properties of amide 79 in these proteins.

The calculated electrostatic effect of reducing the partial charge of amide 79 is of the same order of magnitude as the decrease of the enthalpic component of the reduction potential observed in the S79P variant HiPIP. While it cannot be completely ruled out that the substitution of Ser79 with proline did not induce small changes in the orientation of other main-chain amide groups, the current results provide unequivocal experimental evidence that a single main-chain amide group can contribute as much as 100 mV to the reduction potential of a metalloprotein. The magnitude of this effect, and the difference in the number of properly oriented amide groups surrounding HiPIP and Fd clusters (7 and 13, respectively) suggest that these groups may indeed be the major determinant of the 400–600 mV difference in reduction potential observed between these two families of Fe_4S_4 proteins.

Acknowledgements This work was partially supported by: MURST ex-40%; C.N.R. P.F. Biotecnologie; E.U. contract ERB CHRX-CT94-0626.

References

1. Jensen GM, Warshel A, Stephen PJ (1994) Biochemistry 33:10911–10924
2. Moore GR, Pettigrew GW, Rogers NK (1986) Proc Natl Acad Sci USA 83:4998–4999
3. Bertini I, Borsari M, Bosi M, Eltis LD, Felli IC, Luchinat C, Piccioli M (1996) JBIC 1:257–263
4. Bertini I, Gori Savellini G, Luchinat C (1997) JBIC 2:114–118
5. Capozzi F, Ciurli S, Luchinat C (1998) Struct Bonding 90:127–160
6. Zhou H (1997) JBIC 2:109–113
7. Mauk AG, Moore GR (1997) JBIC 2:119–125
8. Li J, Nelson MR, Peng CY, Bashford D, Noodleman L (1998) J Phys Chem 102:6311–6324
9. Heering HA, Bulsink YBM, Hagen WR, Meyer TE (1995) Biochemistry 34:14675–14686
10. Banci L, Bertini I, Ciurli S, Luchinat C, Pierattelli R (1995) Inorg Chim Acta 240:251–256
11. Banci L, Bertini I, Gori Savellini G, Luchinat C (1996) Inorg Chem 35:4248–4253
12. Swartz PD, Ichiye T (1997) Biophys J 73:2733–2741
13. Denke E, Merbitz-Zahradnik T, Hatzfeld OM, Snyder CH, Link TA, Trumpower BL (1998) J Biol Chem 273:9085–9093
14. Schroter T, Hatzfeld OM, Gemeinhardt S, Korn M, Friedrich T, Ludwig B, Link TA (1998) Eur J Biochem 255:100–106.
15. Heering HA, Bulsink YBM, Hagen WR, Meyer TE (1995) Eur J Biochem 232:811–817
16. Backes G, Mino Y, Loehr TM, Meyer TE, Cusanovich MA, Sweeney WV, Adman ET, Sanders-Loehr J (1991) J Am Chem Soc 113:2055–2064
17. Carter CWJ, Kraut J, Freer ST, Alden RA (1974) J Biol Chem 249:6339–6346
18. Zeng Q, Smith ET, Kurtz DM Jr, Scott RA (1996) Inorg Chim Acta 242:245–251
19. Bertini I, Ciurli S, Luchinat C (1995) Struct Bonding 83:1–54

20. Ausubel FM, Brent R, Kingston RE, Moore DD, Seidman JG, Smith HA, Struhl K (1991) Current protocols in molecular biology. Greene, New York
21. Kunkel TA, Roberts JD, Zakour RA (1987) Methods Enzymol 154:267–382
22. Babini E, Bertini I, Borsari M, Capozzi F, Dikiy A, Eltis LD, Luchinat C (1996) J Am Chem Soc 118:75–80
23. Eltis LD, Iwagami SG, Smith M (1994) Protein Eng 7:1145–1150
24. Bartsch RG (1978) Methods Enzymol 53:329–340
25. Babini E, Borsari M, Capozzi F (1998) Inorg Chim Acta 275–276:230–233
26. Pearlman DA, Case DA, Caldwell JW, Ross WS, Cheatham TE, Ferguson DM, Seibel GL, Singh UC, Weiner PK, Kollman PA (1995) AMBER 4.1. University of California, San Francisco
27. Parisini E, Capozzi F, Lubini P, Lamzin V, Luchinat C, Sheldrick GM (1999) Acta Crystallogr (in press)
28. Koradi R, Billeter M, Wüthrich K (1996) J Mol Graphics 14:51–55
29. Mouesca J-M, Chen JL, Noodleman L, Bashford D, Case DA (1994) J Am Chem Soc 116:11898–11914
30. Banci L, Pierattelli R (1995) In: La Mar GN (ed) Nuclear magnetic resonance of paramagnetic macromolecules. (NATO ASI series) Kluwer, Dordrecht, pp 281–296
31. Agarwal A, Li D, Cowan JA (1995) Proc Natl Acad Sci USA 92:9440–9444
32. Bertini I, Cowan JA, Luchinat C, Natarajan K, Piccioli M (1997) Biochemistry 36:9332–9339
33. Luchinat C, Capozzi F, Borsari M, Battistuzzi G, Sola M (1994) Biochem Biophys Res Commun 203:436–442
34. Bertini I, Capozzi F, Ciurli S, Luchinat C, Messori L, Piccioli M (1992) J Am Chem Soc 114:3332–3340
35. Luchinat C, Ciurli S, Capozzi F (1992) In: Williams AF, Floriani C, Merbach AE (eds) Perspectives in coordination chemistry. VCH, Basel, pp 245–270
36. Banci L, Bertini I, Ferretti S, Luchinat C, Piccioli M (1993) J Mol Struct 292:207–220
37. Bertini I, Capozzi F, Luchinat C, Piccioli M, Vila AJ (1994) J Am Chem Soc 116:651–660
38. Luchinat C, Ciurli S (1993) Biol Magn Reson 12:357–420
39. Bertini I, Capozzi F, Eltis LD, Felli IC, Luchinat C, Piccioli M (1995) Inorg Chem 34:2516–2523
40. Warshel A, Papazyan A, Muegge I (1997) JBIC 2:143–152